

Quantified causality dependence of dynamical relation between zonal flow and heat transport on isotope mass in tokamak edge plasmas

Yu He(何钰), Zhongbing Shi(石中兵), Yuhong Xu(许宇鸿), Jun Cheng(程钧), Jianqiang Xu(许健强), Zhihui Huang(黄治辉), Na Wu(吴娜), Kaiyang Yi(弋开阳), Weice Wang(王威策), Min Jiang(蒋敏), Longwen Yan(严龙文), Xiaoquan Ji(季小全), and Wulyu Zhong(钟武律)

Citation: Chin. Phys. B, 2025, 34 (**10**): 105202. DOI: 10.1088/1674-1056/ade069
http://cpb.iphy.ac.cn; http://iopscience.iop.org/cpb

What follows is a list of articles you may be interested in

Calculation and prediction of divertor detachment via impurity seeding by using one-dimensional model

Wen-Jie Zhou(周文杰), Xiao-Ju Liu(刘晓菊), Xiao-He Wu(邬潇河), Bang Li(李邦), Qi-Qi Shi(石奇奇), Hao-Chen Fan(樊皓尘), Yan-Jie Yang(杨艳杰), and Guo-Qiang Li(李国强)

Chin. Phys. B, 2024, 33 (**8**): 085205. DOI: 10.1088/1674-1056/ad426a

Role of the zonal flow in multi-scale multi-mode turbulence with small-scale shear flow in tokamak plasmas

Hui Li(李慧), Jiquan Li(李继全), Zhengxiong Wang(王正汹), Lai Wei(魏来), and Zhaoqing Hu(胡朝清)

Chin. Phys. B, 2022, 31 (**6**): 065207. DOI: 10.1088/1674-1056/ac6011

The intermittent excitation of geodesic acoustic mode by resonant Instanton of electron drift wave envelope in L-mode discharge near tokamak edge

Zhao-Yang Liu(刘朝阳), Yang-Zhong Zhang(章扬忠), Swadesh Mitter Mahajan, A-Di Liu(刘阿娣), Chu Zhou(周楚), and Tao Xie(谢涛)

Chin. Phys. B, 2022, 31 (**4**): 045202. DOI: 10.1088/1674-1056/ac43ac

Basic features of the multiscale interaction between tearing modes and slab ion-temperature-gradient modes

L Wei(魏来), Z X Wang(王正汹), J Q Li(李继全), Z Q Hu(胡朝清), Y Kishimoto(岸本泰明)

Chin. Phys. B, 2019, 28 (**12**): 125203. DOI: 10.1088/1674-1056/ab5437

Reversed rotation of limit cycle oscillation and dynamics of low-intermediate-high confinement transition

Dan-Dan Cao(曹丹丹), Feng Wan(弯峰), Ya-Juan Hou(侯雅娟), Hai-Bo Sang(桑海波), Bai-Song Xie(谢柏松)

Chin. Phys. B, 2018, 27 (**6**): 065201. DOI: 10.1088/1674-1056/27/6/065201

Quantified causality dependence of dynamical relation between zonal flow and heat transport on isotope mass in tokamak edge plasmas

Yu He(何钰)[1], Zhongbing Shi(石中兵)[1,†], Yuhong Xu(许宇鸿)[2], Jun Cheng(程钧)[2], Jianqiang Xu(许健强)[1], Zhihui Huang(黄治辉)[1], Na Wu(吴娜)[1], Kaiyang Yi(弋开阳)[1], Weice Wang(王威策)[1], Min Jiang(蒋敏)[1], Longwen Yan(严龙文)[1], Xiaoquan Ji(季小全)[1], and Wulyu Zhong(钟武律)[1]

[1] *Southwestern Institute of Physics, Chengdu* 610041, *China*

[2] *Institute of Fusion Science, School of Physical Science and Technology, Southwest Jiaotong University, Chengdu* 610031, *China*

(Received 27 March 2025; revised manuscript received 13 May 2025; accepted manuscript online 4 June 2025)

The isotope effect on zonal flows (ZFs) and turbulence remains a key issue that is not completely solved in fusion plasmas. This paper presents the first experimental results of the *ab initio* prediction of causal relation between geodesic acoustic mode (GAM) and ambient turbulence at different isotope masses in the edge of HL-2A tokamak, where transfer entropy method based on information-theoretical approach is utilized as a quantified indicator of causality. Analysis shows that GAM is more pronounced in deuterium plasmas than in hydrogen, leading to a lower heat transport as well as more peaked profiles in the former situation. The causal impact of GAM on conductive heat flux component is stronger than on the convective component, which is resulted from a larger causal influence of zonal flow on temperature fluctuation. While a stronger GAM in deuterium plasmas has larger influence on all flux components, the relative change in temperature fluctuation and coefficient is more obvious when the ion mass varies. These findings not only offer an in-depth understanding of the real causality between zonal flow and turbulence in the present isotope experiments, but also provide useful ways for the physical understandings of transport and zonal flow dynamics in future deuterium–tritium fusion plasmas.

Keywords: isotope effect, zonal flow, heat transport, causality

PACS: 52.55.Fa, 52.55.–s, 96.50.Tf, 52.35.Kt

DOI: 10.1088/1674-1056/ade069 **CSTR:** 32038.14.CPB.ade069

1. Introduction

The isotope effect has been a long unresolved physics and a major challenge in magnetic confinement fusion research.[1] Although theoretical gyro-Bohm scaling[2] predicts that heavier ions would reduce confinement due to increased radial transport, experiments have demonstrated that deuterium (D) plasmas exhibit longer confinement times compared to hydrogen (H) plasmas under similar conditions.[3–6] This divergence between theoretical predictions and experimental observations induced by isotope mass is typically termed as the "isotope effect". The manifestation of this effect varies across different devices: some experiments reveal a strong positive correlation between ion mass and confinement time, whereas others indicate a weak or negligible dependence.[7–9] Consequently, gaining a comprehensive understanding of the underlying physical mechanisms of the isotope effect is crucial for optimizing plasma performance in future deuterium–tritium (D–T) fusion reactors.

In order to elucidate the physical mechanism of isotope effect on the confinement property, several theories have been proposed,[10–12] with zonal flow (ZF) activity being identified as a leading candidate. Zonal flow is poloidally symmetric large scale structures with finite radial wavenumber generated via nonlinear three-wave interactions by turbulence which can suppress turbulence through flow shearing.[13–15] There are two kinds of ZFs, *i.e.*, the low/zero frequency ZF (L/ZFZF)[16,17] and the high frequency branch geodesic acoustic mode (GAM).[18–20] Whilst the former generally exists in the core and can hardly be recognized in present devices, the latter is more obvious at the edge plasma and is much easier to be detected. Therefore, the edge plasmas characterized by GAM-turbulence system offers a good conditions for studying the basic physics of zonal flow and transport dynamics. For example, studies on TEXTOR provide the first experimental evidence that larger GAM amplitude is associated higher D/H ratio.[21] Subsequent observations on TJ-II corroborated the impact of isotope mass on turbulent structures.[7] These results highlight the critical role of multi-scale interaction between turbulence and ZFs in regulating the observed isotope effects.

Whilst most results indicate that the influence of isotopes on plasma transport and confinement is resulted from the different turbulent and ZF amplitudes, there remain many unresolved physics regarding the mechanisms of the isotopic effect, particularly the direct quantifications of the causality. In this paper, we report the first experimental results of the isotope effect on the nonlinear coupling between zonal flow and temperature fluctuation responsible for the heat transport, combined with a direct information-theoretical-based causal-

†Corresponding author. E-mail: shizb@swip.ac.cn

© 2025 Chinese Physical Society and IOP Publishing Ltd. All rights, including for text and data mining, AI training, and similar technologies, are reserved.

ity analysis of the modulation effect of ZFs on heat transport using transfer entropy technique, which provides an in-depth understanding of complex nonlinear physics of the isotope effect.

2. Experimental results

Experiments were conducted in ohmically heated hydrogen and deuterium plasmas on the HL-2A tokamak[22] (major radius $R = 165$ cm and minor radius $a = 40$ cm). H and D isotope plasmas have similar discharge conditions with line-averaged density $\bar{n}_e \sim 1.3 \times 10^{19}$ m^{-3}, plasma current $I_p \sim 150$ kA and toroidal magnetic field $B_t \sim 1.3$ T. In these experiments, the edge plasma physical parameters were measured by a double-step Langmuir probe array located at the mid-plane on the low-field side, whose innermost radial position is about 3 cm inside the last closed flux surface (LCFS), i.e., $r - r_{LCFS} = -3$ cm, at where the GAM and fluctuations can be clearly detected simultaneously.[23–25] The local electron density (n_e) and temperature (T_e) can be estimated based on the triple-probe principle.[26] The poloidal electric field E_θ can be calculated via two floating potentials (ϕ) measured by poloidally separated pins as $E_\theta = (\phi_1 - \phi_2)/\Delta\theta$ ($\Delta\theta$ is the poloidal distance of the two pins), and then the radial velocity is obtained, $V_r = E_\theta/B_t$. The turbulent particle Γ_r and heat flux Q_r are calculated by $\Gamma_r = \langle\tilde{n}_e\tilde{E}_\theta\rangle/B_t$ and $Q_r = 3/2\langle\tilde{p}_e\tilde{E}_\theta\rangle/B_t$, where the tilde denotes the fluctuation part and bracket denotes the ensemble average, respectively. All the results obtained in this study have excellent reproducibility.

Figure 1 shows the comparison of typical discharge waveforms and edge profiles in H- and D-dominated plasmas. Figures 1(a1)–1(c1) are the plasma current, central line-averaged density, and plasma's stored energy, respectively. It is clearly seen that under the same plasma discharge conditions the stored energy in D plasmas is approximately twice as that in H plasmas, which implies that the heat transport level is much lower in D plasmas. The vertical dashed lines denote the measuring time by Langmuir probe in these experiments, with approximately the same radial position in H and D plasmas thus reducing the impact of location on the turbulence properties. The radial profiles of electron density, electron temperature, and their gradients averaged in several similar discharges in H (blue) and D (red) plasmas are shown in Figs. 1(a2)–1(b2) and 1(a3)–1(b3), respectively. The local electron density in the edge is slightly increased in D plasmas compared with H, leading to the fact that the distinction of electron density gradient profiles (∇n_e) is not obvious, as can be found in Fig. 1(b2). Figure 1(a3) shows the radial profile of electron temperature, where a clear increase in D plasmas is found so that in the edge region temperature gradient (∇T_e) is higher in D plasmas as seen in Fig. 1(b3). The transports in terms of particle and heat fluxes (Γ_r and Q_r) are illustrated in Figs. 1(c2) and 1(c3), respectively. It is observed that both fluxes inside the LCFS are reduced in D plasmas, which is consistent with the higher plasma stored energy observed in D discharges. As a result, it is strongly suggested that the fluxes associated with temperature gradients and its fluctuation play a key role in determining the transport in the edge region.

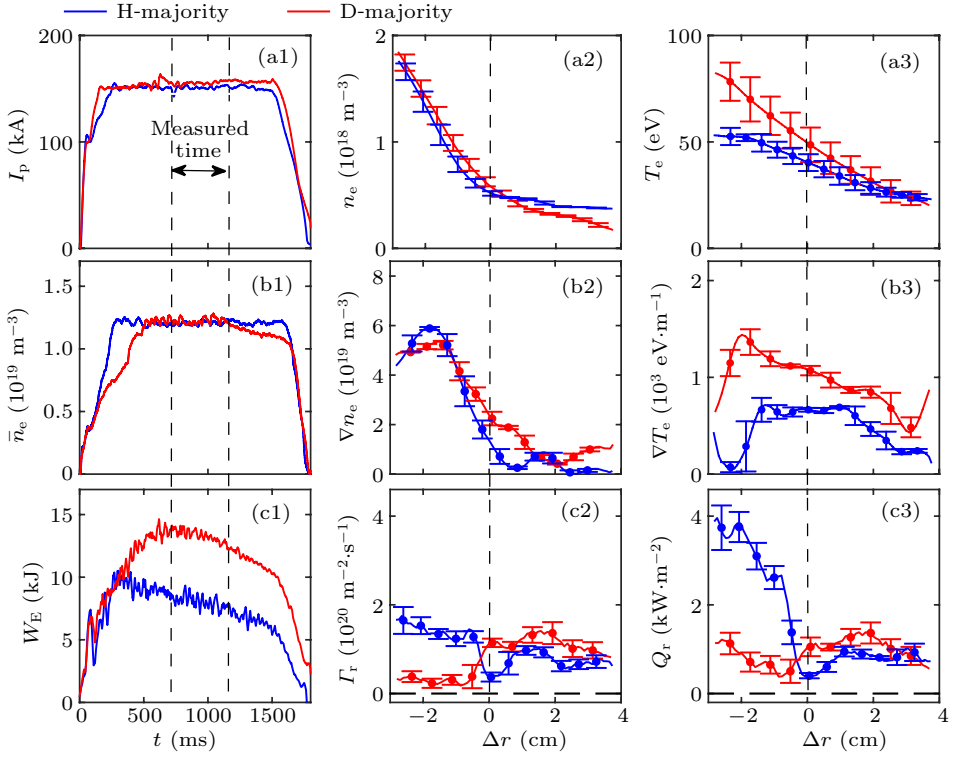


Fig. 1. Time traces of (a1) plasma current, (b1) central line-averaged density, (c1) stored energy. Radial profiles of (a2) electron density, (b2) density gradient, (c2) particle flux, (a3) electron temperature, (b3) temperature gradient and (c3) heat flux. The error bars indicate the standard deviation estimated in several similar shots and the vertical dashed lines in the profile plots denote the last closed flux surface.

A low-frequency coherent mode peaking at around $f \sim 10$ kHz is identified as GAM zonal flow that has been systematic studied on HL-2A for a long time,[19,25,27] and its nonlinear interaction in spectral space between ambient turbulence in isotope discharge experiments has been previously studied in Ref. [28]. In order to explore the impact of the isotope mass on heat flux, the frequency spectra of various fluctuation quantities and their contributions to convective and conductive heat flux components are compared, i.e., $Q = Q_{\rm conv} + Q_{\rm cond} = \frac{3}{2}(T_{\rm e}\langle\tilde{n}_{\rm e}\tilde{V}_{\rm r}\rangle + n_{\rm e}\langle\tilde{T}_{\rm e}\tilde{V}_{\rm r}\rangle)$, which can be normalized by the pressure as $Q_{\rm conv} = \left\langle\frac{\tilde{n}_{\rm e}}{n_{\rm e}}\tilde{V}_{\rm r}\right\rangle$ and $Q_{\rm cond} = \left\langle\frac{\tilde{T}_{\rm e}}{T_{\rm e}}\tilde{V}_{\rm r}\right\rangle$, where $\tilde{n}_{\rm e}$, $\tilde{T}_{\rm e}$, and $\tilde{V}_{\rm r}$ represent the electron density, electron temperature, and radial velocity fluctuations, respectively. Figure 2 depicts the spectra of convective and conductive fluxes, where the former is defined as

$$Q_{\rm conv}(f) = \frac{\left\langle\frac{\tilde{n}_{\rm e}}{n_{\rm e}}(f)\tilde{V}_{\rm r}(f)\right\rangle}{B_t} = \frac{k_\theta(f)\left|[P_{(\tilde{n}_{\rm e}/n_{\rm e})}(f)P_{\tilde{\phi}}(f)\right| \times C_{(\tilde{n}_{\rm e}/n_{\rm e})\tilde{\phi}}(f)}{B_t},$$

in which the coefficient is calculated as

$$C_{(\tilde{n}_{\rm e}/n_{\rm e})\tilde{\phi}} = \sin\alpha_{(\tilde{n}_{\rm e}/n_{\rm e})\tilde{\phi}} P_{(\tilde{n}_{\rm e}/n_{\rm e})\tilde{\phi}} / [P_{(\tilde{n}_{\rm e}/n_{\rm e})} P_{\tilde{\phi}}],$$

and α is the angle between the two signals in frequency space.[29] Likewise the conductive component is defined in the same way. The power spectrum peaks at the GAM frequency as shown in Fig. 2(e). In Figs. 2(d) and 2(h), it is noted that in the low-frequency range ($f < 20$ kHz), both the convective and conductive heat fluxes almost vanish, since the poloidal wave number k_θ of GAM is close zero and it does not drive transport, as shown by Figs. 2(b) and 2(f). In the medium frequency (20 kHz–60 kHz), cross-power and coherence for the convective heat flux do not show significant difference in both isotope plasmas, whereas they have distinct feature regarding the conductive component. It is plausible that the coherence between temperature and potential fluctuations maybe an important reason for the reduction of conductive flux in D plasmas, consequently leading to a substantial decrease in overall heat transport.

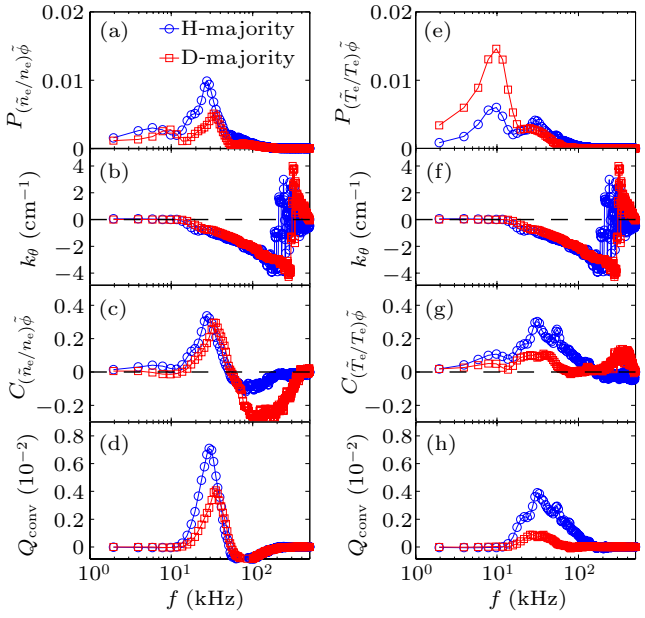


Fig. 2. Frequency spectra of convective (left panel) and conductive (right panel) heat flux. Panels (a) and (e) are the cross-power between $\tilde{n}/n$ ($\tilde{T}_{\rm e}/T_{\rm e}$) and $\tilde{\phi}$; panels (b) and (f) are the poloidal wavenumber spectrum; panels (c) and (g) are the coherence between $\tilde{n}/n$ ($\tilde{T}_{\rm e}/T_{\rm e}$) and $\tilde{\phi}$; panels (d) and (h) are convective and conductive heat flux spectra, respectively.

Although the cross spectrum technique is good for explaining the modulation effect, it is not a measure of the real 'causality' but the similarity in frequency space. This linear analysis falls short in quantifying the strength of causal relationships. Thus, a direct causality analysis should be performed for the understandings isotope effect on zonal flow and its modulation effect on ambient turbulence. Here, a direction causality measuring technique based on information-theoretical approach[30] is introduced, the transfer entropy (TE).[31] Transfer entropy quantifies the enhancement in predicting the next sample of signal X through the utilization of not only its own time history but also that of signal Y, which provides a quantitative framework for assessing causality by measuring the information gained about future events based on past events. Causal interactions are categorized into redundant, unique, and synergistic contributions, depending on their nature. This method is non-intrusive, maintains invariance under invertible variable transformations and is highly suitable for both computational simulations and experimental studies. In a simplified manner, the transfer entropy can be expressed using the following formula:

$$\mathrm{TE}_{Y\to X}(k) = \sum p(x_{N+1}, x_{N-k}, y_{N-k}) \log_2 \frac{p(x_{N+1}|x_{N-k}, y_{N-k})}{p(x_{N+1}|x_{N-k})}.$$

The probability distributions $p(a,b,c,\ldots)$ can be estimated by dividing each argument into m bins, resulting in a total of m^d bins for $p(a,b,c,\ldots)$. Here, d represents the dimension of p. The probability distribution $p(x|y) = p(x,y)/p(y)$ represents the conditional probability distribution of x conditional on y. The length of the signal is denoted as N, and the time-delay embedding vector k can be converted to a 'time lag' by dividing the sampling frequency as $\Delta\tau = k/f_{\rm s}$.[32] The sum in equation runs over the corresponding discrete bins. Low number of bins (here $m = 2$ or 3) are used due to the requirement of course graining in the construction of the probability distributions. By calculating the TE with varying time delays, the temporal scale of the maximum impact of one variable on another can be accurately quantified by the TE value expressed in bits, regardless of their amplitudes or sign. Since its first application for fusion plasmas by Van Milligen *et al.*,[33] it has

become a powerful tool for the investigation of complex interactions and modulation phenomena in the field of tearing modes, zonal flows, and so on.[34–36]

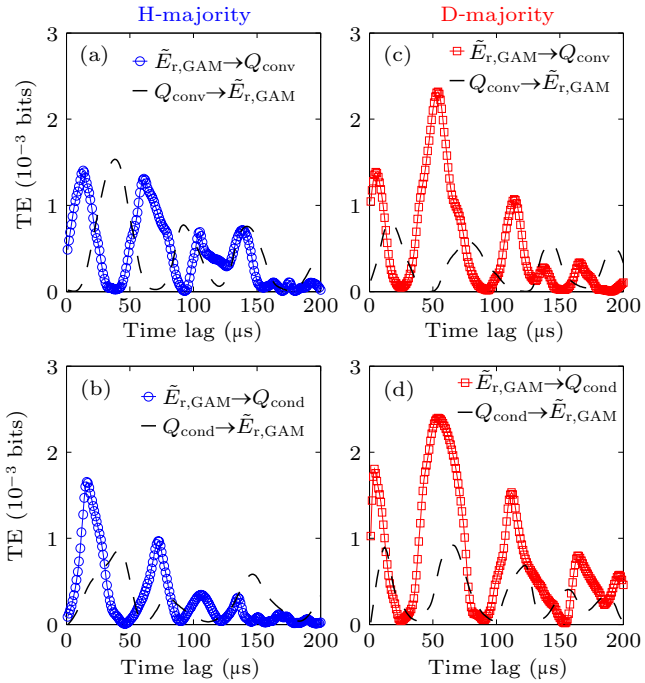


Fig. 3. Transfer entropy between GAM and convective and conductive heat flux in H (left panel) and D (right panel) plasmas. Panels (a) and (c) are the causal relations between GAM and convective component while panels (b) and (d) are that for conductive component, respectively.

In order to have a deeper insight into the intricate causal relationships between the GAM and the heat transport mechanisms of convective and conductive nature, figure 3 shows the calculated transfer entropy values that quantitatively delineate these interactions. Here the GAM is represented by its radial electric field fluctuation $\tilde{E}_{\rm r,GAM}$ bandpass filtered from the $\tilde{E}_{\rm r}$ in the frequency range of 8 kHz–12 kHz which covers the full width at half maximum of the GAM, where $\tilde{E}_{\rm r}$ is calculated by the two potentials measured by the two steps with radial resolution of 2.5 mm. The results elucidate a significant causal linkage between $\tilde{E}_{\rm r,GAM}$ and both the convective and conductive heat flux components for typical H and D plasmas. The observed modulation amplitude represented by TE values in D plasmas markedly exceeds that recorded in H plasmas, indicating a much stronger influence of GAM on heat transport, as can be inferred by the comparison between Figs. 3(a)–3(c) and Figs. 3(b)–3(d). This finding aligns well with previous analysis that the comparatively lower convective and conductive heat fluxes in D plasmas than in H, due to the fact that the stronger GAM as well as its regulation effect is responsible for reduced heat transport processes in the former cases. The modulation effect shows a gradual decay at long time scale due to the intermittent nature of the GAMs.[37–39] By investigating these interactions through the framework of transfer entropy, it is shown that the effective way for optimizing energy flux is essential. Consequently, it is also suggested that exploring the interplay between zonal flows and heat fluxes is vital for understanding the transport features in fusion plasmas.

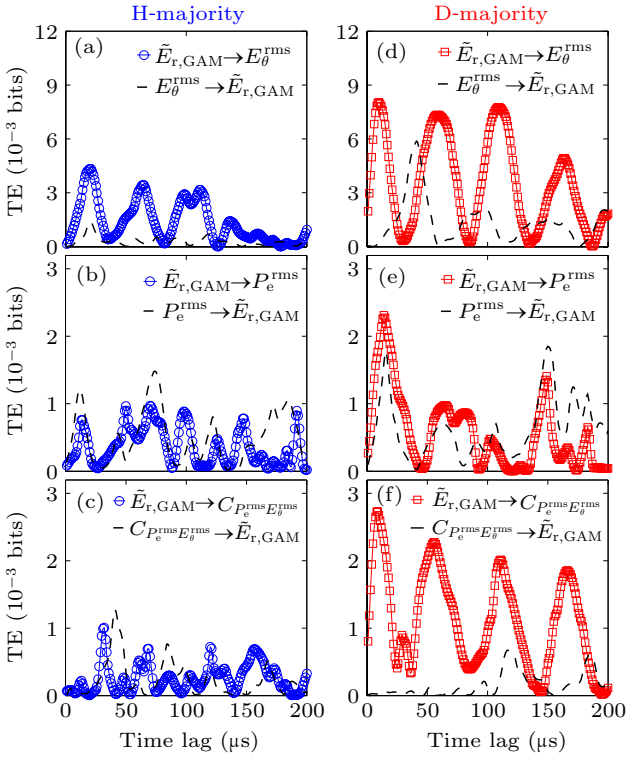


Fig. 4. Transfer entropy between $\tilde{E}_{\rm r,GAM}$ and each component of heat flux. In the left panel, from panels (a)–(c) are the causal relations between $\tilde{E}_{\rm r,GAM}$ and $E_\theta^{\rm rms}$, $P_{\rm e}^{\rm rms}$ and $C_{P_{\rm e}^{\rm rms}E_\theta^{\rm rms}}$ for the case of H plasmas. The corresponding relations for D plasmas are shown in the right panel by panels (d)–(f).

Although the impact of ZF on total transport shows that larger GAM amplitude in D plasmas has stronger influence on turbulence, it is also important for us to understand how GAM affects each flux components, as turbulent heat flux is computed as the product of root-mean square (RMS) of poloidal electric field ($E_\theta^{\rm rms}$), pressure ($P_{\rm e}^{\rm rms}$), and the coherence ($C_{P_{\rm e}^{\rm rms}E_\theta^{\rm rms}}$) between them. According to theory,[26] the coherence is calculated as $C_{P_{\rm e}^{\rm rms}E_\theta^{\rm rms}} = Q_{\rm r}/(P_{\rm e}^{\rm rms}E_\theta^{\rm rms}/B_t) = \langle\tilde{P}_{\rm e}\tilde{E}_\theta/B_{\rm t}\rangle/(P_{\rm e}^{\rm rms}E_\theta^{\rm rms}/B_{\rm t})$. The corresponding causal relation between each component of the heat flux and $\tilde{E}_{\rm r,GAM}$ is illustrated in Fig. 4. It is worth noting that while the causal impact of GAM on $E_\theta^{\rm rms}$ is larger than that on the other two components in both isotopes, the relative change of causal effect of GAM on pressure and coherence is larger than that on the electric field when the ion mass varies. For example, it is seen that the largest $\mathrm{TE}_{\tilde{E}_{\rm r,GAM}\to E_\theta^{\rm rms}}$ values are 0.004 and 0.008 in H and D plasmas, whilst $\mathrm{TE}_{\tilde{E}_{\rm r,GAM}\to C_{P_{\rm e}^{\rm rms}E_\theta^{\rm rms}}}$ are 0.001 and 0.0028, implying that the transport reduction in a heavier ion plasmas is resulted from the larger causal influence on pressure and coherence rather than the potential. It can be seen that $\tilde{E}_{\rm r,GAM}$ has a strong influence on all elements in D plasmas, as can be easily concluded from Figs. 4(a) and 4(d). However, in the H plasmas, $\tilde{E}_{\rm r,GAM}$ only has a significant impact on the

poloidal electric field fluctuations, while no clear relationship is observed between $\tilde{E}_{\mathrm{r,GAM}}$ and either the pressure fluctuation or the coherence, as can be found by larger TE values in Figs. 4(e)–4(f) than that in Figs. 4(b)–4(c). The above results demonstrate that GAM exhibits a stronger modulating effect on coherence in D plasmas, which is consistent with the analysis presented in Figs. 2 and 3.

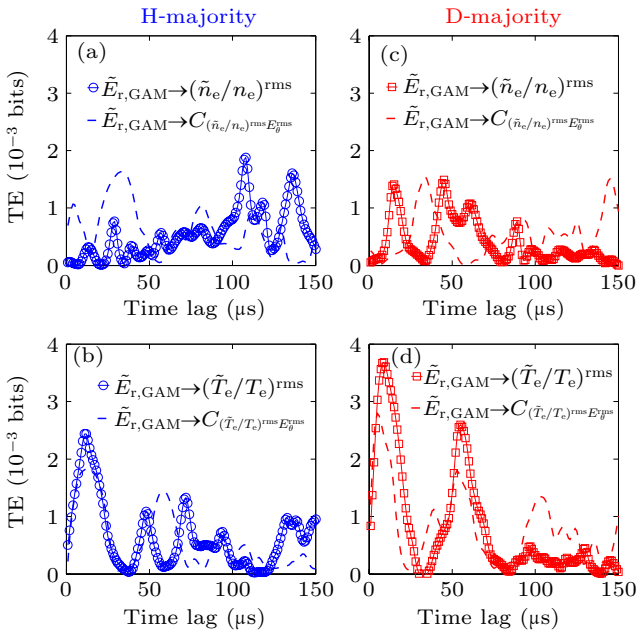


Fig. 5. The transfer entropy between $\tilde{E}_{\mathrm{r,GAM}}$ and $(\tilde{n}_{\mathrm{e}}/n_{\mathrm{e}})^{\mathrm{rms}}$, $(\tilde{T}_{\mathrm{e}}/T_{\mathrm{e}})^{\mathrm{rms}}$, and the correlation coefficients as a function of time lag. Panels (a) and (b) are the causal relations for H plasmas while panels (c) and (d) are those for D plasmas, respectively.

According to the heat flux expression, the transport with different isotope mass is primarily resulted from pressure fluctuations and the correlation coefficient that can be written as $(\tilde{P}_{\mathrm{e}}/P_{\mathrm{e}})^{\mathrm{rms}} = (\tilde{n}_{\mathrm{e}}/n_{\mathrm{e}})^{\mathrm{rms}} + (\tilde{T}_{\mathrm{e}}/T_{\mathrm{e}})^{\mathrm{rms}}$ and $C_{P_{\mathrm{e}}^{\mathrm{rms}}E_{\theta}^{\mathrm{rms}}} = C_{(\tilde{n}_{\mathrm{e}}/n_{\mathrm{e}})^{\mathrm{rms}}E_{\theta}^{\mathrm{rms}}} + C_{(\tilde{T}_{\mathrm{e}}/T_{\mathrm{e}})^{\mathrm{rms}}E_{\theta}^{\mathrm{rms}}}$, which enable us to further investigate the separate causal relationships between $\tilde{E}_{\mathrm{r,GAM}}$ and temperature and density fluctuations as well as the coefficients. In this sense, it can provide an insightful understanding of the isotope effect on heat transport, which is presented in Fig. 5. It is observed that in both H and D plasmas the $\tilde{E}_{\mathrm{r,GAM}}$ has a larger causal impact on both $\tilde{T}_{\mathrm{e}}/T_{\mathrm{e}}$ and $C_{(\tilde{T}_{\mathrm{e}}/T_{\mathrm{e}})^{\mathrm{rms}}E_{\theta}^{\mathrm{rms}}}$ and the modulation amplitude is higher with heavier ion mass, as can be concluded by the comparison between Figs. 5(a) and 5(c) as well as Figs. 5(b) and 5(d). The modulation effects of GAM on temperature fluctuations show a weak periodicity in H plasmas due to the weak GAM activity, as can be inferred from Figs. 5(a) and 5(b). More importantly, it is found that GAM is more important in regulating the coefficients than the fluctuations in both situations, indicating that stronger zonal flow together with its stronger modulation on coefficient between temperature and potential perturbations in D plasmas is the key factor for the reduction of the conductive heat flux, which further leads to a decrease in the overall heat transport, as observed in the present experiments.

3. Summary

The complex effect of isotope mass on edge turbulence and zonal flows, particularly in relation to heat transport, was investigated using spectral analysis and direct causality detection techniques in the HL-2A H/D isotope experiments. The results indicate that deuterium plasmas exhibit stronger GAM zonal flows and lower energy transport compared to hydrogen plasmas. A detailed analysis of the underlying mechanisms reveals a significantly larger coefficient between temperature and potential fluctuations in D plasmas, which is responsible for the reduced thermal conduction flux observed in D plasmas hence contributing to lower total heat flux. Transfer entropy analysis further demonstrates a clear causal relationship between GAM and temperature fluctuations in both H and D plasmas, where in the latter situation a notably higher modulation effect is discovered. These findings highlight the critical role of zonal flows in modulating heat transport processes, particularly through correlation coefficients and temperature fluctuation amplitudes. The study provides valuable insights into the mechanisms behind the isotope effect, which is essential for understanding plasma transport dynamics in the forthcoming deuterium-tritium fusion experiments.

Acknowledgements

The authors thank to the HL-2A team for their operational assistance in the experiments. Project supported by the National MCF Energy Research and Development Program (Grant Nos. 2024YFE03190001, 2024YFE03190004, 2022YFE03030001, and 2019YFE03030002), the National Natural Science Foundation of China (Grant Nos. 12405257, 12475215, and 12475219), the Natural Science Foundation of Sichuan Province, China (Grant Nos. 2023NSFSC1289 and 2025ZNSFSC0066), the Nuclear Technology Research and Development Program (Grant No. HJSYF2024(02)), and the Innovation Program of Southwestern Institute of Physics (Grant No. 202301XWCX001).

References

[1] Bessenrodt-Weberpals M, Wagner F, Gehre O, Giannone L, Hofmann J V, Kallenbach A, Mccormick K, Mertens V, Murmann H D, Ryter F, Scott B D, Siller G, Soldner F X, Stabler A, Steuer K H, Stroth U, Tsois N, Verbeek H and Zoohm H 1993 *Nucl. Fusion* **33** 1205

[2] Manfredi G and Ottaviani M 1997 *Phys. Rev. Lett.* **79** 4190

[3] Saibene G, Horton L D, Sartori R, Balet B, Clement S, Conway G D, Cordey J G, Esch H P L D, Ingesson L C, Lingertat J, Monk R D, Parail V V, Smith R J, Taroni A, Thomsen K and Hellermann M G V 1999 *Nucl. Fusion* **39** 1133

[4] Bose T and Sen A K 2001 *Phys. Plasmas* **8** 4690

[5] Ida K 2023 *Rev. Mod. Plasma Phys.* **7** 23

[6] Yamada H, Tanaka K, Seki R, Suzuki C, Ida K, Fujii K, Goto M, Murakami S, Osakabe M, Tokuzawa T, Yokoyama M, Yoshinuma M and Group L E 2019 *Phys. Rev. Lett.* **123** 185001

[7] Liu B, Pedrosa M A, Van Milligen B P, Hidalgo C, Silva C, Tabarés F L, Zurro B, Mccarthy K J, Cappa A and Liniers M 2015 *Nucl. Fusion* **55** 112002

[8] Lorenzini R and Gobbin M 2021 *Plasma Phys. Control. Fusion* **63** 114005

[9] Maggi C F, Weisen H, Casson F J, Auriemma F, Lorenzini R, Nordman H, Delabie E, Eriksson F, Flanagan J, Keeling D, King D, Horvath L, Menmuir S, Salmi A, Sips G, Tala T and Voitsekhovich I 2019 *Nucl. Fusion* **59** 076028

[10] Hahm T S, Lu W, Wang W X, Yoon E S and Duthoit F X 2013 *Nucl. Fusion* **53** 072002

[11] Watanabe T H, Sugama H and Nunami M 2011 *Nucl. Fusion* **51** 123003

[12] Garcia J, Görler T, Jenko F and Giruzzi G 2017 *Nucl. Fusion* **57** 014007

[13] Diamond P H, Itoh S I, Itoh K and Hahm T S 2005 *Plasma Phys. Control. Fusion* **47** R35

[14] Itoh K, Itoh S I, Diamond P H, Hahm T S, Fujisawa A, Tynan G R, Yagi M and Nagashima Y 2006 *Phys. Plasmas* **13** 055502

[15] Fujisawa A 2009 *Nucl. Fusion* **49** 013001

[16] Lin Z, Hahm T S, Lee W W, Tang W M and White R B 1998 *Science* **281** 1835

[17] Fujisawa A, Itoh K, Iguchi H, Matsuoka K, Okamura S, Shimizu A, Minami T, Yoshimura Y, Nagaoka K, Takahashi C, Kojima M, Nakano H, Ohsima S, Nishimura S, Isobe M, Suzuki C, Akiyama T, Ida K, Toi K, Itoh S I and Diamond P H 2004 *Phys. Rev. Lett.* **93** 165002

[18] Winsor N, Johnson J L and Dawson J M 1968 *Phys. Fluids* **11** 2448

[19] Zhao K J, Lan T, Dong J Q, Yan L W, Hong W Y, Yu C X, Liu A D, Qian J, Cheng J, Yu D L, Yang Q W, Ding X T, Liu Y and Pan C H 2006 *Phys. Rev. Lett.* **96** 255004

[20] Conway G D, Smolyakov A I and Ido T 2022 *Nucl. Fusion* **62** 013001

[21] Xu Y, Hidalgo C, Shesterikov I, Krämer-Flecken A, Zoletnik S, Schoor M V, Vergote M and Team T T 2013 *Phys. Rev. Lett.* **110** 265005

[22] Xu M, Duan X R, Liu Y, *et al.* 2019 *Nucl. Fusion* **59** 112017

[23] Lan T, Liu A D, Yu C X, Yan L W, Hong W Y, Zhao K J, Dong J Q, Qian J, Cheng J, Yu D L and Yang Q W 2008 *Phys. Plasmas* **15** 056105

[24] Lan T, Liu A D, Yu C X, Yan L W, Hong W Y, Zhao K J, Dong J Q, Qian J, Cheng J, Yu D L and Yang Q W 2008 *Plasma Phys. Control. Fusion* **50** 045002

[25] Liu A D, Lan T, Yu C X, Zhao H L, Yan L W, Hong W Y, Dong J Q, Zhao K J, Qian J, Cheng J, Duan X R and Liu Y 2009 *Phys. Rev. Lett.* **103** 095002

[26] Demidov V I, Ratynskaia S V and Rypdal K 2002 *Rev. Sci. Instrum.* **73** 3409

[27] Zhong W L, Shi Z B, Xu Y, Zou X L, Duan X R, Chen W, Jiang M, Yang Z C, Zhang B Y, Shi P W, Liu Z T, Xu M, Song X M, Cheng J, Ke R, Nie L, Cui Z Y, Fu B Z, Ding X T, Dong J Q, Yi L, Yan L W, Yang Q W, Liu Y and Team H A 2015 *Nucl. Fusion* **55** 113005

[28] He Y, Cheng J, Xu Y, Fang Q, Li Y, Xu J, Wang W, Yan L, Huang Z, Wu N, Jiang M, Shi Z, Liu Y, Zhong W and Xu M 2022 *Plasma Sci. Technol.* **24** 095102

[29] Powers E J 1974 *Nucl. Fusion* **14** 749

[30] Hlaváčková-Schindler K, Paluš M, Vejmelka M and Bhattacharya J 2007 *Phys. Rep.* **441** 1

[31] Schreiber T 2000 *Phys. Rev. Lett.* **85** 461

[32] Wibral M, Pampu N, Priesemann V, Siebenhuhner F, Seiwert H, Lindner M, Lizier J T and Vicente R 2013 *PLoS One* **8** e55809

[33] Van Milligen B P, Birkenmeier G, Ramisch M, Estrada T, Hidalgo C and Alonso A 2014 *Nucl. Fusion* **54** 023011

[34] Van Milligen B P, Carreras B A, Voldiner I, Losada U, Hidalgo C and Team T I 2021 *Phys. Plasmas* **28** 092302

[35] Van Milligen B P, Estrada T, Carreras B A, Ascasíbar E, Hidalgo C, Pastor I, Fontdecaba J M, Balbín R and Team T I 2016 *Phys. Plasmas* **23** 072305

[36] Xu J Q, Qu Y R, Li J C, Lin Z, Dong J Q, Peng X D, Jiang M, Qu H P, Huang Z H, Wu N, Wang W C, Hao G Z, Chen W, Li J Q and Xu M 2022 *Nucl. Fusion* **62** 086048

[37] Mckee G R, Gupta D K, Fonck R J, Schlossberg D J, Shafer M W and Gohil P 2006 *Plasma Phys. Control. Fusion* **48** S123

[38] Hillesheim J C, Peebles W A, Carter T A, Schmitz L and Rhodes T L 2012 *Phys. Plasmas* **19** 022301

[39] Gao Z 2013 *Phys. Plasmas* **20** 032501